AMERICAN SOCIETY FOR MICROBIOLOGY | mSystems®

RESEARCH ARTICLE

The Effect of *Limosilactobacillus reuteri* on Social Behavior Is Independent of the Adaptive Immune System

Sean W. Dooling,[a,b,c] Martina Sgritta,[a,b] I-Ching Wang,[a,b] Ana Luiza Rocha Faria Duque,[d] Mauro Costa-Mattioli[a,b,c]

[a]Department of Neuroscience, Baylor College of Medicine, Houston, Texas, USA
[b]Memory and Brain Research Center, Baylor College of Medicine, Houston, Texas, USA
[c]Department of Molecular and Human Genetics, Baylor College of Medicine, Houston, Texas, USA
[d]Department of Food and Nutrition, School of Pharmaceutical Sciences, São Paulo State University (UNESP), Araraquara, Brazil

Sean W. Dooling and Martina Sgritta contributed equally to this article. Author order was determined alphabetically.

ABSTRACT Gut microbes can modulate almost all aspects of host physiology throughout life. As a result, specific microbial interventions are attracting considerable attention as potential therapeutic strategies for treating a variety of conditions. Nonetheless, little is known about the mechanisms through which many of these microbes work. Recently, we and others have found that the commensal bacterium *Limosilactobacillus reuteri* (formerly *Lactobacillus reuteri*) reverses social deficits in several mouse models (genetic, environmental, and idiopathic) for neurodevelopmental disorders in a vagus nerve-, oxytocin-, and biopterin-dependent manner. Given that gut microbes can signal to the brain through the immune system and *L. reuteri* promotes wound healing via the adaptive immune response, we sought to determine whether the prosocial effect mediated by *L. reuteri* also depends on adaptive immunity. Here, we found that the effects of *L. reuteri* on social behavior and related changes in synaptic function are independent of the mature adaptive immune system. Interestingly, these findings indicate that the same microbe (*L. reuteri*) can affect different host phenotypes through distinct mechanisms.

IMPORTANCE Because preclinical animal studies support the idea that gut microbes could represent novel therapeutics for brain disorders, it is essential to fully understand the mechanisms by which gut microbes affect their host's physiology. Previously, we discovered that treatment with *Limosilactobacillus reuteri* selectively improves social behavior in different mouse models for autism spectrum disorder through the vagus nerve, oxytocin reward signaling in the brain, and biopterin metabolites (BH4) in the gut. However, given that (i) the immune system remains a key pathway for host-microbe interactions and that (ii) *L. reuteri* has been shown to facilitate wound healing through the adaptive immune system, we examined here whether the prosocial effects of *L. reuteri* require immune signaling. Unexpectedly, we found that the mature adaptive immune system (i.e., conventional B and T cells) is not required for *L. reuteri* to reverse social deficits and related changes in synaptic function. Overall, these findings add new insight into the mechanism through which *L. reuteri* modulates brain function and behavior. More importantly, they highlight that a given bacterial species can modulate different phenotypes (e.g., wound healing versus social behavior) through separate mechanisms.

KEYWORDS *Limosilactobacillus reuteri*, oxytocin, social behavior, adaptive immune system, gut-microbiota-brain axis, *Lactobacillus reuteri*

Gut microbes are fundamental to nearly every aspect of host physiology and fitness (1, 2), including brain function and behavior. Indeed, a large body of preclinical literature has uncovered a bidirectional communication system linking the gut and the

Editor Suleyman Yildirim, Istanbul Medipol University School of Medicine

Address correspondence to Mauro Costa-Mattioli, costamat@bcm.edu.

The authors declare a conflict of interest. A patent application related to the role of L. reuteri on social behavior has been filed by Baylor College of Medicine. The authors declare no other conflicts of interest.

Received 20 April 2022
Accepted 22 September 2022
Published 26 October 2022

brain, known as the gut-microbiota-brain axis (3–5). Briefly, foundational studies have demonstrated that germ-free mice and mice treated with broad-spectrum antibiotics exhibit behavioral abnormalities, including endophenotypes associated with neurological disorders, such as autism spectrum disorder (ASD) (6–11). In addition, using experimental mouse models, we and others have shown that gut microbes can modulate endophenotypes for complex neurological disorders in a very powerful way (3, 5, 12–14). In particular, social behavior has emerged as an endophenotype that is strongly regulated by the gut-microbiota-brain axis across species (9, 13, 15–18).

Humans with specific neurological disorders, such as ASD, often possess a different gut microbiota composition (19–23) and are often afflicted with gastrointestinal (GI) symptoms. Furthermore, recent studies have shown that microbiota transfer therapy and dietary modulation of the gut microbiota alleviates both GI and behavioral symptoms in children with certain neurological dysfunction, including ASD (24–26). Thus, the gut microbiome is emerging as an important modulator of both brain development/function and complex behaviors, including social behavior.

Originally, we found that treatment with the bacterial species *Limosilactobacillus reuteri* (formerly *Lactobacillus reuteri* [27]) selectively improves social behavior, but not other behavioral abnormalities, in a maternal obesity model (i.e., maternal high-fat diet offspring) (13) for ASD. In subsequent studies, we found that *L. reuteri* promoted social behavior in genetic (*Shank3B*$^{-/-}$ and *Cntnap2*$^{-/-}$), environmental (valproic acid and germ-free), and idiopathic (BTBR) mouse models of social deficits (14, 28). Importantly, and consistent with our results, two independent studies show that *L. reuteri* reversed the social deficits in *Shank3B*$^{-/-}$ mice (29) and BTBR mice (30). Thus, the finding that *L. reuteri* promotes social behavior is strongly supported by numerous, convergent discoveries in several animal models and across different levels of analysis and laboratories.

However, to fully understand how the gut microbiota modulate brain function and behavior, it is necessary to dissect the underlying molecular, cellular, and systems mechanisms. There are several possible ways by which gut microbes can influence the brain. These include (i) vagus nerve signaling (31), (ii) circulation of microbial metabolites through the blood (32, 33), and (iii) modulation of the immune system (34, 35). Our initial mechanistic studies revealed that *L. reuteri* acts in a vagus nerve-dependent manner and rescues social interaction and social interaction-induced synaptic plasticity in the ventral tegmental area (VTA) of ASD mice, but not in oxytocin receptor-deficient mice (14). More recently, we found that *L. reuteri* acts by promoting biopterin metabolite (BH4) levels in the host's gut (28).

A previous study showed that *L. reuteri* facilitates wound healing through the stimulating a subpopulation of T cells as a part of the adaptive immune response (36), a process also involving signaling through the vagus nerve and oxytocin (36). While there appears to be much overlap in the mechanisms through which *L. reuteri* improves social behavior and wound healing (i.e., vagus nerve and oxytocin signaling), it is currently unknown whether the adaptive immune system plays a role in the effects of *L. reuteri* on social behavior. Therefore, we sought to test the hypothesis that the adaptive immune system, namely, conventional adaptive B and T lymphocytes, also mediates the *L. reuteri* prosocial effect.

Using genetic, behavioral, molecular, and electrophysiological approaches in this study, we found that *L. reuteri* reverses the social deficits in a genetic mouse model for ASD lacking mature conventional B and T cells. Accordingly, *L. reuteri* reverses deficits in oxytocin and synaptic potentiation associated with social reward. Thus, the adaptive immune system is not a major contributor to the *L. reuteri*-mediated rescue of social behavior. Consequently, the mechanisms through which a given bacterial species modulates different aspects of host physiology are not fully shared.

RESULTS

***Shank3B*$^{-/-}$ mice exhibit no deficits in adaptive immune system maturation and *L. reuteri* treatment does not affect mature lymphocyte levels.** The gut microbiota play an important role in the host's immune signaling (37). For example, gut microbes can

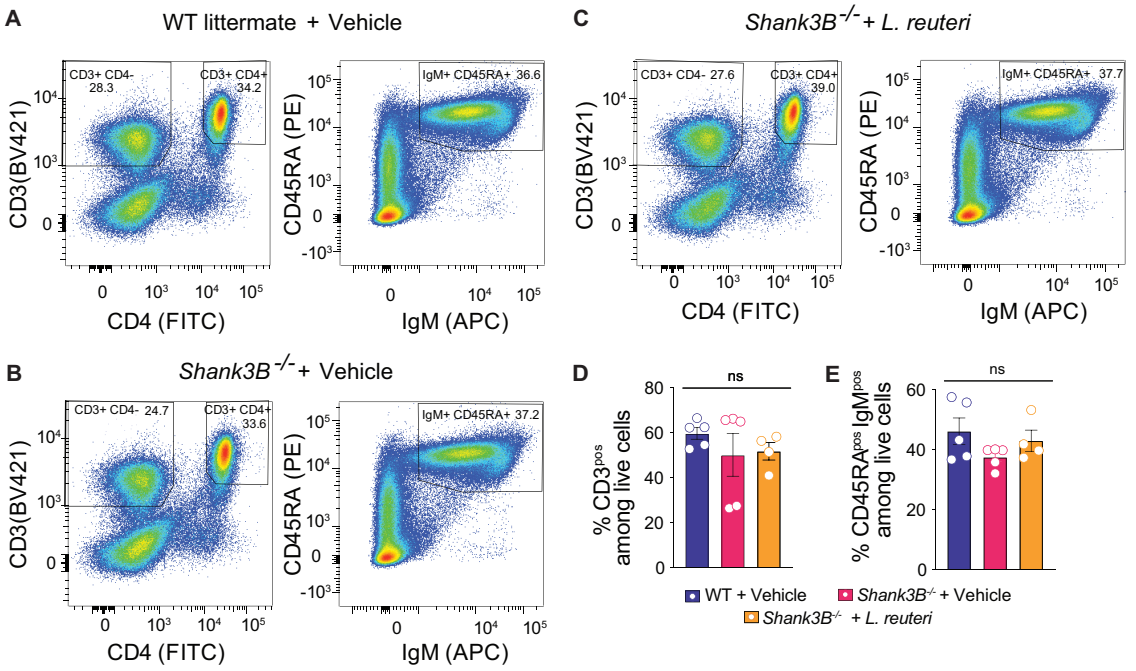

FIG 1 *Shank3B*$^{-/-}$ mice do not show changes in the percentages of mature T and B lymphocytes compared to their controls, and *L. reuteri* does not influence the number of adaptive immune cells. (A to D) Flow cytometry analysis of CD3, CD4, IgM, and CD43RA expression in the spleen cells of WT littermate + vehicle, *Shank3B*$^{-/-}$ + vehicle, and *Shank3B*$^{-/-}$ + *L. reuteri* (n = 4 to 5 mice per group). (A) Distribution of CD3, CD4, IgM, and CD43RA signal in WT littermate + vehicle. (B) Distribution of CD3, CD4, IgM, and CD43RA signal in *Shank3B*$^{-/-}$ + vehicle. (C) Distribution of CD3, CD4, IgM, and CD43RA signal in *Shank3B*$^{-/-}$ + *L. reuteri*. (D) Percentage of all CD3^{+} cells. (WT littermate versus *Shank3B*$^{-/-}$: q = 2.646, P = 0.1929; *Shank3B*$^{-/-}$ versus *Shank3B*$^{-/-}$ + *L. reuteri*: q = 1.576, P = 0.5252; WT littermate versus *Shank3B*$^{-/-}$ + *L. reuteri*: q = 0.9181, P = 0.7966 [one-way ANOVA with Tukey *post hoc* test, P = 0.2131]). (E) Percentage of IgM^{+} and CD43RA^{+} cells. (WT littermate versus *Shank3B*$^{-/-}$: q = 1.544, P = 0.5382; *Shank3B*$^{-/-}$ versus *Shank3B*$^{-/-}$ + *L. reuteri*: q = 0.2462, P = 0.9835; WT littermate versus *Shank3B*$^{-/-}$ + *L. reuteri*: q = 1.210, P = 0.6779 [one-way ANOVA with Tukey *post hoc* test, P = 0.5310]). ns, nonsignificant. Bar graphs show means ± the SEM with individual data points.

modulate immune responses by triggering both proinflammatory (38) and anti-inflammatory responses (39, 40). Interestingly, aberrant immune responses may contribute to some aspects of ASD symptomatology (41), which often features with gastrointestinal comorbidities and alterations in the gut microbiome (42–44).

Specifically, *L. reuteri* has been shown to modulate the adaptive immune system (45–48) and facilitate wound healing (36). However, whether the effect of *L. reuteri* on social behavior also requires the adaptive immune response remains unknown. To answer this question, we used *Shank3B*$^{-/-}$ mouse model for neurodevelopmental disorders because (i) they exhibit social deficits that are reproduced across laboratories (14, 29, 49); (ii) they have a deficient oxytocinergic system (14), which is known to modulate social behaviors and is implicated in ASD (50, 51); and (iii) we and others have previously shown that *L. reuteri* reverses their social deficits (14, 29).

We first examined whether the maturation of the adaptive immune system is altered in *Shank3B*$^{-/-}$ mice compared to control littermates. To this end, we measured the number of T (CD3^{+} CD4^{+} and CD3^{+} CD4^{-}) and B (IgM^{+} and CD43RA^{+}) lymphocytes in control mice, *Shank3B*$^{-/-}$ mice treated with vehicle, and *Shank3B*$^{-/-}$ mice treated with *L. reuteri* using flow cytometry (Fig. 1A to C). We found that there was no significant difference in the percentages of mature T and B lymphocytes between WT control and *Shank3B*$^{-/-}$ mice (Fig. 1D and E). Moreover, *L. reuteri* treatment did not alter the percentages of mature T and B cells in *Shank3B*$^{-/-}$ mice (Fig. 1D and E). Hence, *Shank3B*$^{-/-}$ mice do not exhibit deficits in adaptive immune system maturity, and *L. reuteri* treatment does not affect the overall number of the mature adaptive immune system cells in *Shank3B*$^{-/-}$ mice.

***L. reuteri* treatment corrects social deficits in *Shank3B*$^{-/-}$ mice lacking a mature adaptive immune system.** The deletion of *Rag2* disrupts the formation of the Rag complex and halts B cell and T cell development at the pro-B and the pro-T cell stages

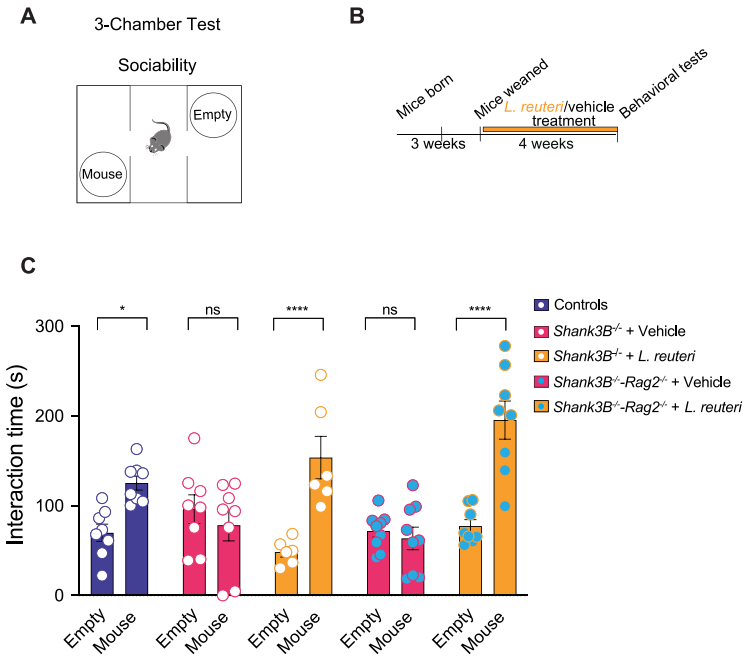

FIG 2 *L. reuteri* corrects social deficits in *Shank3B*$^{-/-}$-*Rag2*$^{-/-}$ mice. (A) Schematic of the three-chamber social behavior test. (B) Schematic of the experimental design. (C) Social interaction in vehicle- and *L. reuteri*-treated WT, *Shank3B*$^{-/-}$, and *Shank3B*$^{-/-}$-*Rag2*$^{-/-}$ mice in the three-chamber test (n = 8 to 9 per group; WT littermate: t = 2.929, P = 0.0194; *Shank3B*$^{-/-}$: t = 0.9491, $P > 0.9999$; *Shank3B*$^{-/-}$ + *L. reuteri*: t = 4.738, $P < 0.0001$; *Shank3B*$^{-/-}$-*Rag2*$^{-/-}$ + vehicle: t = 0.4571, $P > 0.9999$; *Shank3B*$^{-/-}$-*Rag2*$^{-/-}$ + *L. reuteri*: t = 6.247, $P < 0.0001$ [two-way ANOVA with Bonferroni correction, $F_{(4,68)} = 10.34$; $P < 0.0001$]). *, $P < 0.05$; ****, $P < 0.0001$; ns, nonsignificant. Bar graphs show means ± the SEM with individual data points.

prior to V(D)J recombination of B cell and T cell receptors, thus preventing them from reaching full maturation (52). Consequently, *Rag2*$^{-/-}$ mice are a widely used animal model to study deficiencies in adaptive immunity (53–56). We first sought to determine whether genetic ablation of the mature adaptive immune system via the deletion of *Rag2* would alter social behavior. To test social behavior, we performed a three-chamber test for sociability. In this behavioral task (Fig S1A, Fig. 2A), mice can choose either a nonsocial interaction, with an empty cup (Empty), or a social interaction, with an unfamiliar mouse (Mouse). As expected, control (wild-type [WT]) mice display normal social interaction as they spend more time interacting with the mouse instead of the empty cup (Fig S1B). *Rag2*$^{-/-}$ mice also interacted more with the mouse than the cup, indicating that the loss of the Rag2-recombined adaptive immune system does not lead to impaired social behavior.

To test whether *L. reuteri* rescues social behavior in the *Shank3B*$^{-/-}$ mice through modulation of mature B and T cells, we crossed *Shank3B*$^{-/-}$ mice to *Rag2*$^{-/-}$ mice to generate *Shank3B*$^{-/-}$ mice lacking mature B and T lymphocytes, here defined as "*Shank3B*$^{-/-}$-*Rag2*$^{-/-}$" mice. As expected, *Shank3B*$^{-/-}$-*Rag2*$^{-/-}$ mice lack CD3^{+}, CD4^{+}, IgM^{+}, and CD43RA^{+} cells in the spleen, indicating the absence of a mature B and T cells in the mutant mice (see Fig. S2A to D).

Shank3B$^{-/-}$ mice treated with vehicle display social deficits (Fig. 2C), consistent with previous studies (14, 29, 49). Similarly, vehicle-treated *Shank3B*$^{-/-}$-*Rag2*$^{-/-}$ mice also exhibited social deficits (Fig. 2C). If the prosocial effect of *L. reuteri* depends on the adaptive immune system, then *L. reuteri* would fail to rescue the social deficits in *Shank3B*$^{-/-}$-*Rag2*$^{-/-}$ mice. Interestingly, however, we found that *L. reuteri* was able to reverse the social deficits in *Shank3B*$^{-/-}$ mice with a deficient adaptive immune system (*Shank3B*$^{-/-}$-*Rag2*$^{-/-}$ mice) (Fig. 2C). These data demonstrate that *L. reuteri* rescues social behavior independently of the adaptive immune system.

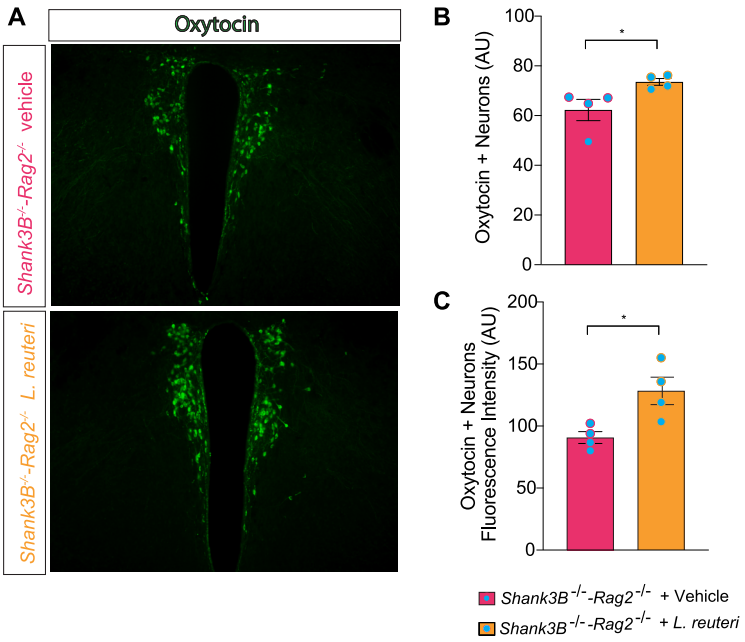

FIG 3 *L. reuteri* increases oxytocin levels in the PVN of the hypothalamus in *Shank3B*$^{-/-}$ *Rag2*$^{-/-}$ mice. (A) Oxytocin immunoreactivity in the PVN of *Shank3B*$^{-/-}$-*Rag2*$^{-/-}$ mice treated with either vehicle or *L. reuteri*. (B) Oxytocin-positive cell (n = 4 mice per group; *Shank3B*$^{-/-}$-*Rag2*$^{-/-}$ + vehicle versus *Shank3B*$^{-/-}$-*Rag2*$^{-/-}$ + *L. reuteri* [unpaired t test, t = 2.519, P = 0.0453]). (C) Oxytocin immunofluorescence intensity (n = 4 mice per group; *Shank3B*$^{-/-}$-*Rag2*$^{-/-}$ + vehicle versus *Shank3B*$^{-/-}$-*Rag2*$^{-/-}$ + *L. reuteri* [unpaired t test, t = 3.124, P = 0.0205]). *, $P < 0.05$. Bar graphs show means ± the SEM with individual data points.

***L. reuteri* treatment increases oxytocin levels in the paraventricular nucleus of *Shank3B*$^{-/-}$ mice lacking a mature adaptive immune system.** Oxytocin (Oxt) is an evolutionarily conserved neuropeptide critically implicated in social behavior (57). Accordingly, several animal models with abnormal social behavior, including *Shank3B*-deficient animals, feature decreased Oxt levels and Oxt treatment rescues select deficits in behavior and brain development in these mice (13, 14, 28, 58–62). In addition, Oxt has been shown to be intricately linked to immune system signaling (63, 64). Interestingly, the effects of *L. reuteri* on both social behavior and wound healing have been shown to be dependent on Oxt signaling (13, 28, 36). Indeed, *L. reuteri* increases Oxt levels in plasma and in the brain of several mouse models of ASD, including *Shank3B*$^{-/-}$ mice (13, 14, 28, 36).

Given that *L. reuteri* reversed the social deficits in *Shank3B*$^{-/-}$ mice with an impaired adaptive immune system, we next examined whether disruptions of the adaptive immune system affect *L. reuteri*'s ability to boost the host's oxytocin system. To this end, we performed immunohistochemistry in paraventricular nucleus (PVN) of the hypothalamus, where Oxt is primarily produced. Consistent with the behavioral data, we found that treatment with *L. reuteri* was able to increase oxytocin levels in *Shank3B*$^{-/-}$-*Rag2*$^{-/-}$ mice, as determined by an increased number and fluorescence intensity of Oxt-positive neurons in the mutant mice treated with *L. reuteri* (Fig. 3). Thus, the adaptive immune system does not affect the *L. reuteri*-mediated increase in Oxt.

***L. reuteri* treatment corrects social interaction-induced synaptic potentiation in the dopaminergic neurons of the ventral tegmental area of *Shank3B*$^{-/-}$ mice lacking a mature adaptive immune system.** Brain regions that process naturally rewarding stimuli are crucially required for social behaviors (65, 66). During social interaction, oxytocin is released from neurons in the PVN and signal to oxytocin receptors on dopaminergic (DA) neurons in the ventral tegmental area (VTA), leading to the release of dopamine and facilitation of a rewarding sensation (67). We and others found that social interaction leads to an increase in synaptic potentiation in VTA DA neurons of

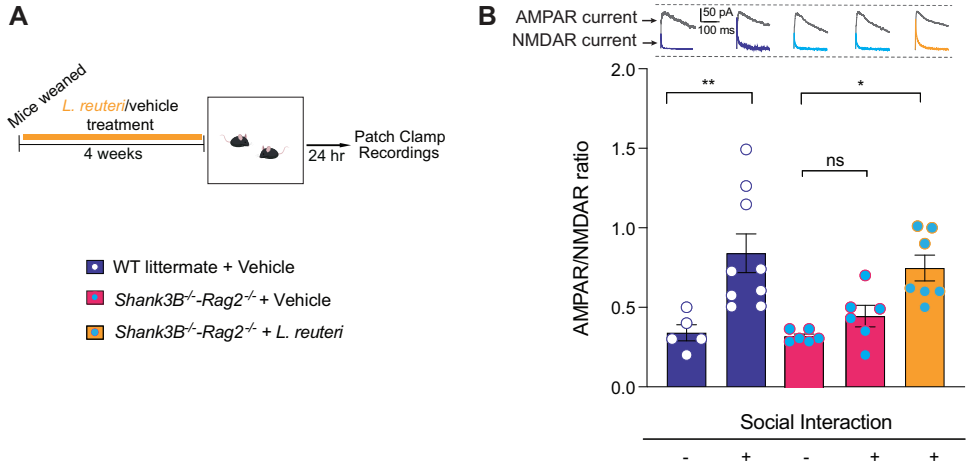

FIG 4 *L. reuteri* restores social interaction-induced synaptic transmission in the DA neurons of the lateral VTA in *Shank3B*$^{-/-}$-*Rag2*$^{-/-}$ mice. (A) Schematic of the experimental design. (B) Representative traces of AMPAR and NMDAR currents (top) and AMPAR/NMDAR ratio (bottom) in dopaminergic neurons of the lateral VTA in baseline condition or following social interaction with a stranger mouse. (n = 5 to 9 mice per group; Control baseline versus Control + stranger interaction: q = 5.396, P = 0.0057; Control baseline versus *Shank3B*$^{-/-}$-*Rag2*$^{-/-}$ baseline: q = 0.1656, $P > 0.9999$; Control baseline versus *Shank3B*$^{-/-}$-*Rag2*$^{-/-}$ + *L. reuteri* + stranger interaction: q = 4.185, P = 0.0452; Control baseline versus *Shank3B*$^{-/-}$-*Rag2*$^{-/-}$ + stranger interaction: q = 1.044, P = 0.9457; Control + stranger interaction versus *Shank3B*$^{-/-}$-*Rag2*$^{-/-}$ baseline: q = 5.900 P = 0.0023; Control + stranger interaction versus *Shank3B*$^{-/-}$-*Rag2*$^{-/-}$ + *L. reuteri* + stranger interaction: q = 1.110, P = 0.9329; Control stranger interaction versus *Shank3B*$^{-/-}$-*Rag2*$^{-/-}$ + stranger interaction: q = 4.511, P = 0.0266; *Shank3B*$^{-/-}$-*Rag2*$^{-/-}$ baseline versus *Shank3B*$^{-/-}$-*Rag2*$^{-/-}$ + *L. reuteri* + stranger interaction: q = 4.585, P = 0.0235; *Shank3B*$^{-/-}$-*Rag2*$^{-/-}$ baseline versus *Shank3B*$^{-/-}$-*Rag2*$^{-/-}$ + stranger interaction: q = 1.268, P = 0.8957; *Shank3B*$^{-/-}$-*Rag2*$^{-/-}$ + *L. reuteri* + stranger interaction versus *Shank3B*$^{-/-}$-*Rag2*$^{-/-}$ + stranger interaction: q = 3.268, P = 0.1712 [one-way ANOVA with Tukey test, $F_{4,28}$ = 7.230, P = 0.0004]). *, $P < 0.05$; **, $P < 0.01$; ns, not significant. Bar graphs show means ± the SEM with individual data points.

both birds and mice (13, 68, 69). Moreover, this evolutionarily conserved process, a likely cellular model of social reward, is impaired in several mouse models for ASD (13, 14, 28). In humans with ASD, magnetic resonance imaging studies have shown deficiencies in the activity of reward regions after social behavior, further supporting the notion that reward centers of the brain are a major regulator of social behavior (70–72). More importantly, we have previously shown that *L. reuteri* reverses the deficits in synaptic potentiation underlying social reward in several mouse models for ASD (13, 14, 28) in an oxytocin-dependent manner (14). Moreover, we found that the *L. reuteri*-induced metabolite, BH4, also corrected changes in social interaction-induced synaptic potentiation (28). However, the role of the adaptive immune system has yet to be explored in this reward-related process.

To determine whether the adaptive immune system was involved in social reward processes, we performed whole-cell patch-clamp recordings and measured the ratio of currents generated by AMPA (α-amino-3-hydroxy-5-methyl-4-isoxazolepropionic acid) and NMDA (*N*-methyl-D-aspartate) receptors (AMPAR/NMDAR ratio) in dopaminergic neurons (Fig. 4A). As expected and consistent with previous results (13, 14, 28), social interaction triggered a significant increase in the AMPAR/NMDAR ratio in WT control mice (Fig. 4B), but it failed to do so in vehicle-treated *Shank3B*$^{-/-}$-*Rag2*$^{-/-}$ mice. The lack of a significant increase in the AMPAR/NMDAR ratio after social interaction indicates impairments in synaptic transmission associated with social reward. Interestingly, *L. reuteri* treatment reverses the deficits in synaptic plasticity in VTA DA neurons from *Shank3B*$^{-/-}$-*Rag2*$^{-/-}$ mice (Fig. 4B).

Taken together these results provide strong evidence that even in the absence of a mature adaptive immune response, *L. reuteri* can reverse the deficits in (i) oxytocin production in the brain, (ii) social behavior, and (iii) social interaction-induced synaptic transmission. Thus, the prosocial effects mediated by *L. reuteri* are independent of the adaptive immune system.

DISCUSSION

Gut microbiota are emerging as a potent modulator brain function and behavior. However, one of the biggest challenges in gut-microbiota-brain axis research remains the identification of the mechanism(s) by which a given bacterial strain regulates a selective behavior or disease state. To understand the precise mechanism(s) through which gut microbes exert their function(s) in the brain can not only help the design of new clinical trials but could also lead to the development of microbe-based, more personalized treatments while minimizing off-target effects.

Our previous work shows that *L. reuteri* improves social behavior in mouse models for ASD through a mechanism involving biopterin (BH4) signaling in the gut, the vagus nerve, and the oxytocinergic-dopaminergic reward circuitry in the brain (13, 14, 28). Here, using genetic, molecular, behavioral, and electrophysiological approaches, we found that *L. reuteri* does not require the mature adaptive immune system to improve social behavior in a mouse model for ASD. Accordingly, *L. reuteri* was able to increase oxytocin levels in the brain and promote synaptic plasticity associated with social reward in the absence of a mature adaptive immune system. These data are unexpected since (i) gut microbes are required for proper development and maturation of the immune system (73); (ii) a majority of immune cells are found in the gut, highlighting the importance of microbe-immune cell interactions (74); and (iii) specifically, *L. reuteri* facilitates wound healing via the vagus nerve, oxytocin, and the adaptive immune system (36).

While our work shows that the Rag2-mediated mature adaptive immune system is not involved in the *L. reuteri*-mediated rescue of social deficits, it remains unknown whether other components of the immune system, such as the innate immune response, could be involved. Indeed, gut microbes and microbial products are known to interact with other immune cells types such as macrophages (75, 76), dendritic cells (77, 78), and innate-like T cells such as mucosal associated invariant T cells (79, 80). These cells could act upstream of oxytocin, vagus nerve, or BH4 signaling and play a role in the rescue of social behavior. However, this has proven challenging to study thus far given limitations in the genetic tools available to specifically ablate these cells *in vivo*.

It is also possible that *L. reuteri* improves social behavior independently of immune cells. For example, *L. reuteri*, or a metabolite produced by *L. reuteri*, could interact with epithelial cells in the gastrointestinal tract to either induce production of BH4 or prevent its degradation. Indeed, gut microbes and their metabolites interact with intestinal epithelial cells (81), which express the enzymes required for BH4 synthesis (82). In addition, specific subtypes of epithelial cells, such as enteroendocrine cells, have been shown to stimulate the vagus nerve (83). Interestingly, BH4 has been shown to stimulate the vagus nerve independent of its role as a cofactor for neurotransmitter synthesis (84). Moreover, BH4 has been shown to increase oxytocin release in neurons (85, 86).

In addition, metabolites produced by *L. reuteri* could directly interact with either enteric nerves or vagal afferent nerves which innervate the intestines (87). For instance, *L. reuteri* has been shown to produce γ-aminobutyrate (GABA) which is one of the nervous system's main signaling molecules (88). Future work will aim to understand whether potential interactions between the *L. reuteri* and/or its metabolites and the innate immune system, intestinal epithelial cells, and/or peripheral nerves affect various phenotypes such as social behavior.

In conclusion, our data presented in this study indicate that *L. reuteri* improves social behavior independently of the mature adaptive immune system and that the bacteria modulate disparate host phenotypes (wound healing and social behaviors) and organs (skin and brain) through different mechanisms.

MATERIALS AND METHODS

Animals. C57BL/6J (stock no. 000664), *Shank3B*$^{+/-}$ (stock no. 017688) (49), and *Rag2*$^{-/-}$ (stock no. 008449) (52) mice were obtained from Jackson Laboratories (Bar Harbor, ME). *Shank3B*$^{-/-}$ mice were generated from *Shank3B*$^{+/-}$ $\times$ *Shank3B*$^{+/-}$ breeding, and littermates were cohoused according to sex.

Shank3B$^{-/-}$-*Rag2*$^{-/-}$ mice were generated by crossing *Shank3B*$^{-/-}$ mice to *Rag2*$^{-/-}$ mice to yield *Shank3B*$^{+/-}$-*Rag2*$^{+/-}$ mice, which were then crossed together to yield double-knockout mice and WT controls. Littermates were cohoused by sex. All mice were kept on a 12-h light/dark cycle and had access to food and water *ad libitum*. Only male mice were included in the study, since we previously found that female *Shank3B*$^{-/-}$ mice display normal social behavior (data not shown). All mice used in these experiments were 7 to 12 weeks of age. Animal care and experimental procedures were approved by Baylor College of Medicine's Institutional Animal Care and Use Committee in accordance with all guidelines set forth by the U.S. National Institutes of Health.

Culture and treatment with *L. reuteri*. *Limosilactobacillus reuteri* 6475 was cultured anaerobically in MRS broth at 37°C in a 90% N_2/5% CO_2/5% H_2 environment as previously described (13, 28). Cultures were centrifuged, washed, resuspended in phosphate-buffered saline (PBS), and frozen at −80°C until use. PBS (vehicle) or *L. reuteri* (~1×10^8 CFU/mouse/day) was added to the drinking water daily. Mice consumed the treated water *ad libitum* for the duration of the treatment period. Behavioral assays, tissue collection, and electrophysiological recordings were initiated 4 weeks after treatment began.

Three-chamber test for social behavior. The three-chamber test for social behavior was assayed on 7- to 10-week-old male mice, as previously described (13, 89). Briefly, mice were first habituated for 10 min an empty 60 × 40 × 23-cm Plexiglass arena divided into three interconnected chambers. Sociability was evaluated during a second 10-min period. The subject could interact either with an empty wire cup (Empty) or a wire cup containing a genotype, age, sex, and treatment-matched stranger conspecific (Mouse). The interaction time was determined by measuring the time the subject mouse spent sniffing or climbing upon either the empty cup or the cup containing the stranger mouse. The empty cup/stranger mouse's position in the left or right chamber during the sociability period was counterbalanced between trials to avoid bias. The time spent interacting with the empty cup or the mouse was recorded and measured using the automated AnyMaze software by trained, independent observers. The human observer was blind to treatment and genotype during the experiment. Preference for social novelty, which is often measured during the three-chamber test, was not performed since we previously found that *Shank3B*$^{-/-}$ mice show a normal preference for social novelty (14).

Flow cytometry. Single cell suspensions were prepared using a GentleMACs dissociator (Miltenyi). Spleens were placed whole into C tubes (Miltenyi) containing 3 mL of digestion buffer and RPMI 1640 (Gibco) containing 100 μg/mL DNase I (Sigma) and 500 μg/mL collagenase IV (Sigma). Organs were ground on the dissociator, incubated 15 min at 25°C, ground again, incubated an additional 15 min, and ground one final time. The homogenates were chilled on ice and enzymes deactivated using 10 mM EDTA. The suspensions were filtered through a 40-mm cell strainer for staining, followed by red blood cell (RBC) lysis using eBioscience RBC lysis solution (Thermo Fisher) for 5 min on ice. The homogenates (1/16 of each spleen) were then Fc-blocked using 4 μg/mL anti-CD16/CD32 antibodies (BD Bioscience Biosciences) on ice for 15 min. Antibody staining was performed for 30 min at 4°C. The following fluorescent anti-mouse antibodies were used: CD3 (BV421, dilution 1/100), CD4+FITC (dilution 1/800), IgM (APC, dilution 1/50), and CD45RA (PE, dilution 1/200). DAPI (4′,6′-diamidino-2-phenylindole; 50 μL/3 mL) staining was used to discriminate between living and dead cells.

The flow cytometric data were then analyzed using FlowJo software (BD Bioscience), including the FlowAI plugin. First, FlowAI (2.0) was run to exclude signal acquisition and dynamic range anomalies using the default settings. Second, debris were excluded based on forward scatter (FSC) and side scatter (SSC). Third and fourth, singlets were isolated using FSC-A versus FSC-H, followed by SSC-W versus SSC-H. Fifth, dead cells were exclude based on the DAPI signal. The various immune cell populations were then isolated by using the various immune markers. In particular, the number of mature T lymphocytes was assessed by measuring $CD3^+$ $CD4^+$ cells and $CD3^+$ $CD4^-$ cells, and the number of mature B lymphocytes was analyzed based on IgM and $CD43RA^+$ expression.

Immunofluorescence. Immunofluorescence was performed as we previously described (13). Briefly, mice were deeply anesthetized by inhalation of isoflurane and perfused through the ascending aorta with 10 mL of 0.9% PBS, followed by 30 mL of 4% paraformaldehyde in 0.1 M phosphate buffer (PB). Brains were removed, immersed in the same fixative overnight at 4°C, and subsequently cryoprotected in 30% sucrose (in 0.1 M PB) over 3 days. Coronal sections were cut at 30 μm with a cryostat (Leica Biosystem) and then collected in ice-cold PBS. Slices were rinsed in 0.1 M PB, blocked with 5% normal goat serum plus 0.3% Triton X-100 0.1 M PB (PBTgs) for 1 h of rocking at room temperature, and then incubated for 24 h at 4°C in a mixture of primary antibodies diluted in PBTgs. Sections were then washed (three times with 0.3% Triton X-100 0.1 M PB), incubated in a mixture of secondary antibodies coupled to a fluorochrome, and diluted in PBTgs for 1.5 to 2 h in the dark at room temperature. Sections were rewashed (three times with PBTgs, 0.1 M PB, and 0.05 M PB, respectively, for 5 min each). Slices were mounted onto 2% gelatin-coated slides (Sigma-Aldrich), air-dried, and cover-slipped with a mounting medium (Fluorescence Vectashield H-1200 with DAPI [Vector Labs]). The primary antibodies used were rabbit anti-oxytocin (ImmunoStar, 1:2,000 dilution), while the secondary antibodies were goat anti-rabbit Alexa Fluor 488 (Thermo Fisher Scientific).

Fluorescent imaging and data acquisition were performed on a Zeiss AxioImager Z2 microscope (Carl Zeiss MicroImaging) mounted with an AxioCam digital camera (Carl Zeiss MicroImaging). Images were captured using AxioVision acquisition software (Carl Zeiss MicroImaging). All images within the same set of experiments were acquired at identical exposure times for every channel used to compare fluorescence intensity. Hypothalamic oxytocin-expressing neurons and NeuN-expressing cell numbers were assessed in the well-defined PVN region using the automatic cell counter plugin in ImageJ, as previously described (14), using the following operational sequence: open image file, 16-bit conversion, subtract background, adjust threshold, watershed, and analyze particles. Automatic identification of cell

boundaries was validated against the source image. Fluorescence intensity was measured in ImageJ by selecting regions of interest (i.e., oxytocin-positive hypothalamic cell bodies, 30 cells per mouse) using the following operational sequence: open image file, 16-bit conversion, set measurement, ROI manager, and measure. Contrast and brightness were linearly adjusted using Photoshop (Adobe) or ImageJ (NIH) uniformly across all images within the data set.

Electrophysiology. Recordings were performed as previously described (13, 90), with minor modifications. Briefly, animals were anesthetized with isoflurane and then decapitated. The brain was rapidly removed from the skull and fixed on a vibroslicer stage (VT 1000S; Leica Microsystems, Buffalo Grove, IL) with cyano-acrylic glue. Acute 220- to 300-μm-thick coronal slices were cut in ice-cold (2 to 3°C) cutting solution containing the following: 87 mM NaCl, 25 mM $NaHCO_3$, 25 mM glucose, 75 mM sucrose, 2.5 mM KCl, 1.25 mM NaH_2PO_4, 0.5 mM $CaCl_2$, and 7 mM $MgCl_2$ (equilibrated with a 95% O_2/5% CO_2) gas mixture (pH 7.3 to 7.5). Slices were incubated for 20 min at 32°C and then stored at room temperature in a holding bath containing oxygenated standard artificial cerebrospinal fluid (ACSF) containing 125 mM NaCl, 25 mM $NaHCO_3$, 25 mM glucose, 2.5 mM KCl, 1.25 mM NaH_2PO_4, 2 mM $CaCl_2$, and 1 mM $MgCl_2$ (equilibrated with 95% O_2/5% CO_2) for at least 40 min before being transferred to a recording chamber mounted on the stage of an upright microscope (Examiner D1; Carl Zeiss, Oberkochen, Germany). The slices were perfused with oxygenated ACSF (2 mL/min) containing the $GABA_A$ receptor antagonist picrotoxin (100 μM; Sigma-Aldrich, USA) and maintained at 32°C with a Peltier feedback device (TC-324B; Warner Instrument). Whole-cell recordings were performed using conventional patch-clamp techniques. Patch pipettes were pulled from borosilicate glass capillaries (World Precision Instruments, Inc., FL) and filled with the following intracellular solution: 117 mM $CsMeSO_3$, 0.4 mM EGTA, 20 mM HEPES, 2.8 mM NaCl, 2.5 mM Mg-ATP, and 0.25 mM Na-GTP. Then, 5 mM Tetraethylammonium Chloride (TEA Cl) was added, the pH was adjusted to 7.3, and the osmolarity was adjusted to 290 mOsm using a Vapro5600 vapor pressure osmometer (ELITechGroup Wescor, South Logan, UT). When filled with the intracellular solution, patch pipettes had a resistance of 2.0 to 3.0 MΩ before seal formation.

Recordings were performed with Multiclamp 700B (Molecular Devices), sampled at 20 kHz with Digidata 1440A (Molecular Devices) interface, filtered online at 3 kHz with a Bessel low-pass filter, and analyzed offline with pClamp10 software (Molecular Devices). The ventral tegmental area (VTA) was visually identified by infrared differential interference contrast video microscopy, and the lateral VTA was determined considering the medial lemniscus and the medial terminal nucleus of the accessory optic tract as anatomical landmarks. Dopaminergic (DA) neurons in this area were identified evaluating the following features: (i) cells firing at a frequency of 1 to 5 Hz and a spike width of >1 ms in a cell-attached configuration, (ii) a membrane capacitance (Cm) of >28 pF, and (iii) the presence of an Ih current and a leak current of >150 pA, when hyperpolarized from −40 mV to −120 in 10-mV steps (91, 92). Passive electrode-cell parameters were monitored throughout the experiments, analyzing passive current relaxations induced by 10-mV hyperpolarizing steps applied at the beginning of every trace. A variation of series resistance (R_s) of >20% led to the rejection of the experiment. AMPAR/NMDAR ratios were calculated as previously described (13, 90). Briefly, neurons were slowly voltage-clamped at +40 mV until the holding current stabilized (at 200 pA). Monosynaptic excitatory postsynaptic currents (EPSC) were evoked at 0.05 Hz with a bipolar stimulating electrode placed 50 to 150 μm rostral to the lateral VTA. After recording the dual-component EPSC, DL-AP5 (100 μM) was bath applied for 10 min to isolate the AMPAR current, blocking the NMDAR. The NMDAR component was then obtained by offline subtraction of the AMPAR component from the original EPSC. The peak amplitudes of the isolated components were used to calculate the AMPAR/NMDAR ratios.

Statistical analysis. Statistical analysis was performed as previously described (14, 28). Data are presented as means ± the standard errors of the mean (SEM). Statistical analyses performed include the unpaired Student *t* test and one- or two-way analysis of variance (ANOVA) with either Tukey's or Bonferroni test to correct for multiple comparisons as indicated in the figure legends, unless otherwise indicated. *P*, *t*, q, and F values are presented in the figure legends. $P < 0.05$ was considered statistically significant (*, $P < 0.05$; **, $P < 0.01$; ***, $P < 0.001$; ****, $P < 0.0001$). Prism 9 software (GraphPad, La Jolla, CA) was used to perform statistical analyses and generate graphical data representations.

Data availability. All data supporting the findings of this study are available within this article and its supplemental material.

SUPPLEMENTAL MATERIAL

Supplemental material is available online only.

FIG S1, EPS file, 1.9 MB.

FIG S2, EPS file, 2.6 MB.

ACKNOWLEDGMENTS

We thank Marina Grasso and Leslie Lopez for administrative support.

This work was supported by funding from NIH (R01MH112356-01), Wellcome Leap, Simons Foundation Autism Research Initiative (SFARI), and by generous support from the Sammons Enterprise to M.C.-M. A.L.R.F.D. was supported by São Paulo Research Foundation (FAPESP) grant 2018/26645-1.

A patent application related to the role of *L. reuteri* on social behavior has been filed by Baylor College of Medicine. We declare no other conflicts of interest.

REFERENCES

1. Backhed F, Ley RE, Sonnenburg JL, Peterson DA, Gordon JI. 2005. Host-bacterial mutualism in the human intestine. Science 307:1915–1920. https://doi.org/10.1126/science.1104816.
2. Bordenstein SR, Theis KR. 2015. Host biology in light of the microbiome: ten principles of holobionts and hologenomes. PLoS Biol 13:e1002226. https://doi.org/10.1371/journal.pbio.1002226.
3. Sharon G, Sampson TR, Geschwind DH, Mazmanian SK. 2016. The central nervous system and the gut microbiome. Cell 167:915–932. https://doi.org/10.1016/j.cell.2016.10.027.
4. Borre YE, O'Keeffe GW, Clarke G, Stanton C, Dinan TG, Cryan JF. 2014. Microbiota and neurodevelopmental windows: implications for brain disorders. Trends Mol Med 20:509–518. https://doi.org/10.1016/j.molmed.2014.05.002.
5. Vuong HE, Yano JM, Fung TC, Hsiao EY. 2017. The microbiome and host behavior. Annu Rev Neurosci 40:21–49. https://doi.org/10.1146/annurev-neuro-072116-031347.
6. Heijtz RD, Wang S, Anuar F, Qian Y, Björkholm B, Samuelsson A, Hibberd ML, Forssberg H, Pettersson S. 2011. Normal gut microbiota modulates brain development and behavior. Proc Natl Acad Sci U S A 108:3047–3052. https://doi.org/10.1073/pnas.1010529108.
7. Arentsen T, Raith H, Qian Y, Forssberg H, Heijtz RD. 2015. Host microbiota modulates development of social preference in mice. Microb Ecol in Health and Dis 26:29719.
8. Neufeld KM, Kang N, Bienenstock J, Foster JA. 2011. Reduced anxiety-like behavior and central neurochemical change in germ-free mice. Neurogastroenterol Motil 23:255–264. https://doi.org/10.1111/j.1365-2982.2010.01620.x.
9. Desbonnet L, Clarke G, Shanahan F, Dinan T, Cryan J. 2014. Microbiota is essential for social development in the mouse. Mol Psychiatry 19:146–148. https://doi.org/10.1038/mp.2013.65.
10. Bercik P, Denou E, Collins J, Jackson W, Lu J, Jury J, Deng Y, Blennerhassett P, Macri J, McCoy KD, Verdu EF, Collins SM. 2011. The intestinal microbiota affect central levels of brain-derived neurotropic factor and behavior in mice. Gastroenterology 141:599–609. https://doi.org/10.1053/j.gastro.2011.04.052.
11. Leclercq S, Mian FM, Stanisz AM, Bindels LB, Cambier E, Ben-Amram H, Koren O, Forsythe P, Bienenstock J. 2017. Low-dose penicillin in early life induces long-term changes in murine gut microbiota, brain cytokines, and behavior. Nat Commun 8:15062. https://doi.org/10.1038/ncomms15062.
12. Sherwin E, Bordenstein SR, Quinn JL, Dinan TG, Cryan JF. 2019. Microbiota and the social brain. Science 366:eaar2016. https://doi.org/10.1126/science.aar2016.
13. Buffington SA, Di Prisco GV, Auchtung TA, Ajami NJ, Petrosino JF, Costa-Mattioli M. 2016. Microbial reconstitution reverses maternal diet-induced social and synaptic deficits in offspring. Cell 165:1762–1775. https://doi.org/10.1016/j.cell.2016.06.001.
14. Sgritta M, Dooling SW, Buffington SA, Momin EN, Francis MB, Britton RA, Costa-Mattioli M. 2019. Mechanisms underlying microbial-mediated changes in social behavior in mouse models of autism spectrum disorder. Neuron 101:246–259.e246. https://doi.org/10.1016/j.neuron.2018.11.018.
15. Venu I, Durisko Z, Xu J, Dukas R. 2014. Social attraction mediated by fruit flies' microbiome. J Exp Biol 217:1346–1352. https://doi.org/10.1242/jeb.099648.
16. Chen K, Luan X, Liu Q, Wang J, Chang X, Snijders AM, Mao J-H, Secombe J, Dan Z, Chen J-H, Wang Z, Dong X, Qiu C, Chang X, Zhang D, Celniker SE, Liu X. 2019. *Drosophila* histone demethylase KDM5 regulates social behavior through immune control and gut microbiota maintenance. Cell Host Microbe 25:537–552.e538. https://doi.org/10.1016/j.chom.2019.02.003.
17. Zhang Z, Mu X, Cao Q, Shi Y, Hu X, Zheng H. 2020. Honeybee gut microbiota modulates host behaviors and neurological processes. bioRxiv. https://www.biorxiv.org/content/10.1101/2020.12.19.423587v1.
18. Wang X, Zheng Y, Zhang Y, Li J, Zhang H, Wang H. 2016. Effects of β-diketone antibiotic mixtures on behavior of zebrafish (*Danio rerio*). Chemosphere 144:2195–2205. https://doi.org/10.1016/j.chemosphere.2015.10.120.
19. Vuong HE, Hsiao EY. 2017. Emerging roles for the gut microbiome in autism spectrum disorder. Biol Psychiatry 81:411–423. https://doi.org/10.1016/j.biopsych.2016.08.024.
20. Ding HT, Taur Y, Walkup JT. 2017. Gut microbiota and autism: key concepts and findings. J Autism Dev Disord 47:480–489. https://doi.org/10.1007/s10803-016-2960-9.
21. Iglesias-Vazquez L, Van Ginkel Riba G, Arija V, Canals J. 2020. Composition of gut microbiota in children with autism spectrum disorder: a systematic review and meta-analysis. Nutrients 12:792. https://doi.org/10.3390/nu12030792.
22. Bundgaard-Nielsen C, Knudsen J, Leutscher PDC, Lauritsen MB, Nyegaard M, Hagstrom S, Sorensen S. 2020. Gut microbiota profiles of autism spectrum disorder and attention deficit/hyperactivity disorder: a systematic literature review. Gut Microbes 11:1172–1187. https://doi.org/10.1080/19490976.2020.1748258.
23. Dan Z, Mao X, Liu Q, Guo M, Zhuang Y, Liu Z, Chen K, Chen J, Xu R, Tang J, Qin L, Gu B, Liu K, Su C, Zhang F, Xia Y, Hu Z, Liu X. 2020. Altered gut microbial profile is associated with abnormal metabolism activity of autism spectrum disorder. Gut Microbes 11:1246–1267. https://doi.org/10.1080/19490976.2020.1747329.
24. Kang D-W, Adams JB, Gregory AC, Borody T, Chittick L, Fasano A, Khoruts A, Geis E, Maldonado J, McDonough-Means S, Pollard EL, Roux S, Sadowsky MJ, Lipson KS, Sullivan MB, Caporaso JG, Krajmalnik-Brown R. 2017. Microbiota transfer therapy alters gut ecosystem and improves gastrointestinal and autism symptoms: an open-label study. Microbiome 5:10. https://doi.org/10.1186/s40168-016-0225-7.
25. Grimaldi R, Gibson GR, Vulevic J, Giallourou N, Castro-Mejia JL, Hansen LH, Leigh Gibson E, Nielsen DS, Costabile A. 2018. A prebiotic intervention study in children with autism spectrum disorders (ASDs). Microbiome 6:133. https://doi.org/10.1186/s40168-018-0523-3.
26. Kang DW, Adams JB, Coleman DM, Pollard EL, Maldonado J, McDonough-Means S, Caporaso JG, Krajmalnik-Brown R. 2019. Long-term benefit of microbiota transfer therapy on autism symptoms and gut microbiota. Sci Rep 9:5821. https://doi.org/10.1038/s41598-019-42183-0.
27. Zheng J, Wittouck S, Salvetti E, Franz CMAP, Harris HMB, Mattarelli P, O'Toole PW, Pot B, Vandamme P, Walter J, Watanabe K, Wuyts S, Felis GE, Gänzle MG, Lebeer S. 2020. A taxonomic note on the genus Lactobacillus: description of 23 novel genera, emended description of the genus *Lactobacillus* Beijerinck 1901, and union of *Lactobacillaceae* and Leuconostocaceae. Int J Syst Evol Microbiol 70:2782–2858. https://doi.org/10.1099/ijsem.0.004107.
28. Buffington SA, Dooling SW, Sgritta M, Noecker C, Murillo OD, Felice DF, Turnbaugh PJ, Costa-Mattioli M. 2021. Dissecting the contribution of host genetics and the microbiome in complex behaviors. Cell 184:1740–1756. https://doi.org/10.1016/j.cell.2021.02.009.
29. Tabouy L, Getselter D, Ziv O, Karpuj M, Tabouy T, Lukic I, Maayouf R, Werbner N, Ben-Amram H, Nuriel-Ohayon M, Koren O, Elliott E. 2018. Dysbiosis of microbiome and probiotic treatment in a genetic model of autism spectrum disorders. Brain Behav Immun 73:310–319. https://doi.org/10.1016/j.bbi.2018.05.015.
30. Nettleton JE, Klancic T, Schick A, Choo AC, Cheng N, Shearer J, Borgland SL, Rho JM, Reimer RA. 2021. Prebiotic, probiotic, and synbiotic consumption alter behavioral variables and intestinal permeability and microbiota in BTBR mice. Microorganisms 9:1833. https://doi.org/10.3390/microorganisms9091833.
31. Bravo JA, Forsythe P, Chew MV, Escaravage E, Savignac HM, Dinan TG, Bienenstock J, Cryan JF. 2011. Ingestion of *Lactobacillus* strain regulates emotional behavior and central GABA receptor expression in a mouse via the vagus nerve. Proc Natl Acad Sci U S A 108:16050–16055. https://doi.org/10.1073/pnas.1102999108.
32. Olson CA, Vuong HE, Yano JM, Liang QY, Nusbaum DJ, Hsiao EY. 2018. The gut microbiota mediates the anti-seizure effects of the ketogenic diet. Cell 173:1728–1741. https://doi.org/10.1016/j.cell.2018.04.027.
33. Blacher E, Bashiardes S, Shapiro H, Rothschild D, Mor U, Dori-Bachash M, Kleimeyer C, Moresi C, Harnik Y, Zur M, Zabari M, Brik RB-Z, Kviatcovsky D, Zmora N, Cohen Y, Bar N, Levi I, Amar N, Mehlman T, Brandis A, Biton I, Kuperman Y, Tsoory M, Alfahel L, Harmelin A, Schwartz M, Israelson A, Arike L, Johansson MEV, Hansson GC, Gotkine M, Segal E, Elinav E. 2019. Potential roles of gut microbiome and metabolites in modulating ALS in mice. Nature 572:474–480. https://doi.org/10.1038/s41586-019-1443-5.
34. Morais LH, Schreiber HL, IV, Mazmanian SK. 2021. The gut microbiota-brain axis in behaviour and brain disorders. Nat Rev Microbiol 19:241–255. https://doi.org/10.1038/s41579-020-00460-0.
35. Regen T, Isaac S, Amorim A, Núñez NG, Hauptmann J, Shanmugavadivu A, Klein M, Sankowski R, Mufazalov IA, Yogev N, Huppert J, Wanke F, Witting M, Grill A, Gálvez EJC, Nikolaev A, Blanfeld M, Prinz I, Schmitt-Kopplin P, Strowig T, Reinhardt C, Prinz M, Bopp T, Becher B, Ubeda C, Waisman A. 2021. IL-17 controls central nervous system autoimmunity through the intestinal microbiome. Sci Immunol 6:eaaz6563. https://doi.org/10.1126/sciimmunol.aaz6563.

36. Poutahidis T, Kearney SM, Levkovich T, Qi P, Varian BJ, Lakritz JR, Ibrahim YM, Chatzigiagkos A, Alm EJ, Erdman SE. 2013. Microbial symbionts accelerate wound healing via the neuropeptide hormone oxytocin. PLoS One 8:e78898. https://doi.org/10.1371/journal.pone.0078898.
37. Rooks MG, Garrett WS. 2016. Gut microbiota, metabolites, and host immunity. Nat Rev Immunol 16:341–352. https://doi.org/10.1038/nri.2016.42.
38. Lee YK, Menezes JS, Umesaki Y, Mazmanian SK. 2011. Proinflammatory T-cell responses to gut microbiota promote experimental autoimmune encephalomyelitis. Proc Natl Acad Sci U S A 108:4615–4622. https://doi.org/10.1073/pnas.1000082107.
39. Matsumoto S, Hara T, Hori T, Mitsuyama K, Nagaoka M, Tomiyasu N, Suzuki A, Sata M. 2005. Probiotic Lactobacillus-induced improvement in murine chronic inflammatory bowel disease is associated with the down-regulation of proinflammatory cytokines in lamina propria mononuclear cells. Clin Exp Immunol 140:417–426. https://doi.org/10.1111/j.1365-2249.2005.02790.x.
40. Kanai T, Mikami Y, Hayashi A. 2015. A breakthrough in probiotics: *Clostridium butyricum* regulates gut homeostasis and anti-inflammatory response in inflammatory bowel disease. J Gastroenterol 50:928–939. https://doi.org/10.1007/s00535-015-1084-x.
41. Ashwood P, Van de Water J. 2004. A review of autism and the immune response. Clin Dev Immunol 11:165–174. https://doi.org/10.1080/10446670410001722096.
42. Finegold SM, Dowd SE, Gontcharova V, Liu C, Henley KE, Wolcott RD, Youn E, Summanen PH, Granpeesheh D, Dixon D, Liu M, Molitoris DR, Green JA. 2010. Pyrosequencing study of fecal microflora of autistic and control children. Anaerobe 16:444–453. https://doi.org/10.1016/j.anaerobe.2010.06.008.
43. Zou R, Xu F, Wang Y, Duan M, Guo M, Zhang Q, Zhao H, Zheng H. 2020. Changes in the gut microbiota of children with autism spectrum disorder. Autism Res 13:1614–1625. https://doi.org/10.1002/aur.2358.
44. Strati F, Cavalieri D, Albanese D, De Felice C, Donati C, Hayek J, Jousson O, Leoncini S, Renzi D, Calabrò A, De Filippo C. 2017. New evidences on the altered gut microbiota in autism spectrum disorders. Microbiome 5:24–24. https://doi.org/10.1186/s40168-017-0242-1.
45. Schepper JD, Collins FL, Rios-Arce ND, Raehtz S, Schaefer L, Gardinier JD, Britton RA, Parameswaran N, McCabe LR. 2019. Probiotic *Lactobacillus reuteri* prevents postantibiotic bone loss by reducing intestinal dysbiosis and preventing barrier disruption. J Bone Miner Res 34:681–698. https://doi.org/10.1002/jbmr.3635.
46. Collins FL, Rios-Arce ND, Schepper JD, Jones AD, Schaefer L, Britton RA, McCabe LR, Parameswaran N. 2019. Beneficial effects of *Lactobacillus reuteri* 6475 on bone density in male mice is dependent on lymphocytes. Sci Rep 9:14708. https://doi.org/10.1038/s41598-019-51293-8.
47. Cervantes-Barragan L, Chai JN, Tianero MD, Di Luccia B, Ahern PP, Merriman J, Cortez VS, Caparon MG, Donia MS, Gilfillan S, Cella M, Gordon JI, Hsieh C-S, Colonna M. 2017. *Lactobacillus reuteri* induces gut intraepithelial $CD4^+$ $CD8\alpha\alpha^+$ T cells. Science 357:806–810. https://doi.org/10.1126/science.aah5825.
48. Karimi K, Inman MD, Bienenstock J, Forsythe P. 2009. *Lactobacillus reuteri*-induced regulatory T cells protect against an allergic airway response in mice. Am J Respir Crit Care Med 179:186–193. https://doi.org/10.1164/rccm.200806-951OC.
49. Peça J, Feliciano C, Ting JT, Wang W, Wells MF, Venkatraman TN, Lascola CD, Fu Z, Feng G. 2011. Shank3 mutant mice display autistic-like behaviours and striatal dysfunction. Nature 472:437–442. https://doi.org/10.1038/nature09965.
50. Donaldson ZR, Young LJ. 2008. Oxytocin, vasopressin, and the neurogenetics of sociality. Science 322:900–904. https://doi.org/10.1126/science.1158668.
51. LoParo D, Waldman ID. 2015. The oxytocin receptor gene (OXTR) is associated with autism spectrum disorder: a meta-analysis. Mol Psychiatry 20:640–646. https://doi.org/10.1038/mp.2014.77.
52. Hao Z, Rajewsky K. 2001. Homeostasis of peripheral B cells in the absence of B cell influx from the bone marrow. J Exp Med 194:1151–1164. https://doi.org/10.1084/jem.194.8.1151.
53. Shinkai Y, Rathbun G, Lam K-P, Oltz EM, Stewart V, Mendelsohn M, Charron J, Datta M, Young F, Stall AM. 1992. RAG-2-deficient mice lack mature lymphocytes owing to inability to initiate V_DJ rearrangement. Cell 68:855–867. https://doi.org/10.1016/0092-8674(92)90029-C.
54. Lu K, Knutson CG, Wishnok JS, Fox JG, Tannenbaum SR. 2012. Serum metabolomics in a *Helicobacter hepaticus* mouse model of inflammatory bowel disease reveal important changes in the microbiome, serum peptides, and intermediary metabolism. J Proteome Res 11:4916–4926. https://doi.org/10.1021/pr300429x.
55. Yates F, Malassis-Séris M, Stockholm D, Bouneaud C, Larousserie F, Noguiez-Hellin P, Danos O, Kohn DB, Fischer A, de Villartay J-P, Cavazzana-Calvo M. 2002. Gene therapy of RAG-$2^{-/-}$ mice: sustained correction of the immunodeficiency. Blood 100:3942–3949. https://doi.org/10.1182/blood-2002-03-0782.
56. Garrett WS, Gallini CA, Yatsunenko T, Michaud M, DuBois A, Delaney ML, Punit S, Karlsson M, Bry L, Glickman JN, Gordon JI, Onderdonk AB, Glimcher LH. 2010. *Enterobacteriaceae* act in concert with the gut microbiota to induce spontaneous and maternally transmitted colitis. Cell Host Microbe 8:292–300. https://doi.org/10.1016/j.chom.2010.08.004.
57. Ross HE, Young LJ. 2009. Oxytocin and the neural mechanisms regulating social cognition and affiliative behavior. Front Neuroendocrinol 30:534–547. https://doi.org/10.1016/j.yfrne.2009.05.004.
58. Harony-Nicolas H, Kay M, Hoffmann J d, Klein ME, Bozdagi-Gunal O, Riad M, Daskalakis NP, Sonar S, Castillo PE, Hof PR, Shapiro ML, Baxter MG, Wagner S, Buxbaum JD. 2017. Oxytocin improves behavioral and electrophysiological deficits in a novel *Shank3*-deficient rat. Elife 6:e18904. https://doi.org/10.7554/eLife.18904.
59. Reichova A, Bacova Z, Bukatova S, Kokavcova M, Meliskova V, Frimmel K, Ostatnikova D, Bakos J. 2020. Abnormal neuronal morphology and altered synaptic proteins are restored by oxytocin in autism-related SHANK3 deficient model. Mol Cell Endocrinol 518:110924. https://doi.org/10.1016/j.mce.2020.110924.
60. Peñagarikano O, Lázaro MT, Lu X-H, Gordon A, Dong H, Lam HA, Peles E, Maidment NT, Murphy NP, Yang XW, Golshani P, Geschwind DH. 2015. Exogenous and evoked oxytocin restores social behavior in the Cntnap2 mouse model of autism. Sci Transl Med 7:271ra278. https://doi.org/10.1126/scitranslmed.3010257.
61. Dai Y-C, Zhang H-F, Schön M, Böckers TM, Han S-P, Han J-S, Zhang R. 2018. Neonatal oxytocin treatment ameliorates autistic-like behaviors and oxytocin deficiency in valproic acid-induced rat model of autism. Front Cell Neurosci 12:355. https://doi.org/10.3389/fncel.2018.00355.
62. Resendez SL, Namboodiri VMK, Otis JM, Eckman LEH, Rodriguez-Romaguera J, Ung RL, Basiri ML, Kosyk O, Rossi MA, Dichter GS, Stuber GD. 2020. Social stimuli induce activation of oxytocin neurons within the paraventricular nucleus of the hypothalamus to promote social behavior in male mice. J Neurosci 40:2282–2295. https://doi.org/10.1523/JNEUROSCI.1515-18.2020.
63. Li T, Wang P, Wang SC, Wang Y-F. 2016. Approaches mediating oxytocin regulation of the immune system. Front Immunol 7:693. https://doi.org/10.3389/fimmu.2016.00693.
64. Wang P, Yang H-P, Tian S, Wang L, Wang SC, Zhang F, Wang Y-F. 2015. Oxytocin-secreting system: a major part of the neuroendocrine center regulating immunologic activity. J Neuroimmunol 289:152–161. https://doi.org/10.1016/j.jneuroim.2015.11.001.
65. Gunaydin LA, Grosenick L, Finkelstein JC, Kauvar IV, Fenno LE, Adhikari A, Lammel S, Mirzabekov JJ, Airan RD, Zalocusky KA, Tye KM, Anikeeva P, Malenka RC, Deisseroth K. 2014. Natural neural projection dynamics underlying social behavior. Cell 157:1535–1551. https://doi.org/10.1016/j.cell.2014.05.017.
66. Dölen G, Darvishzadeh A, Huang KW, Malenka RC. 2013. Social reward requires coordinated activity of nucleus accumbens oxytocin and serotonin. Nature 501:179–184. https://doi.org/10.1038/nature12518.
67. Hung LW, Neuner S, Polepalli JS, Beier KT, Wright M, Walsh JJ, Lewis EM, Luo L, Deisseroth K, Dölen G, Malenka RC. 2017. Gating of social reward by oxytocin in the ventral tegmental area. Science 357:1406–1411. https://doi.org/10.1126/science.aan4994.
68. Bariselli S, Hörnberg H, Prévost-Solié C, Musardo S, Hatstatt-Burklé L, Scheiffele P, Bellone C. 2018. Role of VTA dopamine neurons and neuroligin 3 in sociability traits related to nonfamiliar conspecific interaction. Nat Commun 9:3173. https://doi.org/10.1038/s41467-018-05382-3.
69. Huang Y-C, Hessler NA. 2008. Social modulation during songbird courtship potentiates midbrain dopaminergic neurons. PLoS One 3:e3281. https://doi.org/10.1371/journal.pone.0003281.
70. Supekar K, Kochalka J, Schaer M, Wakeman H, Qin S, Padmanabhan A, Menon V. 2018. Deficits in mesolimbic reward pathway underlie social interaction impairments in children with autism. Brain 141:2795–2805. https://doi.org/10.1093/brain/awy191.
71. Richey JA, Rittenberg A, Hughes L, Damiano CR, Sabatino A, Miller S, Hanna E, Bodfish JW, Dichter GS. 2014. Common and distinct neural features of social and non-social reward processing in autism and social anxiety disorder. Soc Cogn Affect Neurosci 9:367–377. https://doi.org/10.1093/scan/nss146.

72. Kohls G, Perino MT, Taylor JM, Madva EN, Cayless SJ, Troiani V, Price E, Faja S, Herrington JD, Schultz RT. 2013. The nucleus accumbens is involved in both the pursuit of social reward and the avoidance of social punishment. Neuropsychologia 51:2062–2069. https://doi.org/10.1016/j.neuropsychologia.2013.07.020.
73. Round JL, Mazmanian SK. 2009. The gut microbiota shapes intestinal immune responses during health and disease. Nat Rev Immunol 9:313–323. https://doi.org/10.1038/nri2515.
74. Faria AMC, Weiner HL. 2005. Oral tolerance. Immunol Rev 206:232–259. https://doi.org/10.1111/j.0105-2896.2005.00280.x.
75. Plüddemann A, Mukhopadhyay S, Gordon S. 2006. The interaction of macrophage receptors with bacterial ligands. Expert Rev Mol Med 8:1–25. https://doi.org/10.1017/S1462399406000159.
76. Ivec M, Botić T, Koren S, Jakobsen M, Weingartl H, Cencič A. 2007. Interactions of macrophages with probiotic bacteria lead to increased antiviral response against vesicular stomatitis virus. Antiviral Res 75:266–274. https://doi.org/10.1016/j.antiviral.2007.03.013.
77. Niess JH, Reinecker H-C. 2006. Dendritic cells in the recognition of intestinal microbiota. Cell Microbiol 8:558–564. https://doi.org/10.1111/j.1462-5822.2006.00694.x.
78. Tytgat HLP, van Teijlingen NH, Sullan RMA, Douillard FP, Rasinkangas P, Messing M, Reunanen J, Satokari R, Vanderleyden J, Dufrêne YF, Geijtenbeek TBH, de Vos WM, Lebeer S. 2016. Probiotic gut microbiota isolate interacts with dendritic cells via glycosylated heterotrimeric pili. PLoS One 11:e0151824. https://doi.org/10.1371/journal.pone.0151824.
79. Chiba A, Murayama G, Miyake S. 2018. Mucosal-associated invariant T cells in autoimmune diseases. Front Immunol 9:1333. https://doi.org/10.3389/fimmu.2018.01333.
80. Krause JL, Schäpe SS, Schattenberg F, Müller S, Ackermann G, Rolle-Kampczyk UE, Jehmlich N, Pierzchalski A, von Bergen M, Herberth G. 2020. The activation of mucosal-associated invariant T (MAIT) cells is affected by microbial diversity and riboflavin utilization *in vitro*. Front Microbiol 11:755. https://doi.org/10.3389/fmicb.2020.00755.
81. Solis AG, Klapholz M, Zhao J, Levy M. 2020. The bidirectional nature of microbiome-epithelial cell interactions. Curr Opin Microbiol 56:45–51. https://doi.org/10.1016/j.mib.2020.06.007.
82. Haber AL, Biton M, Rogel N, Herbst RH, Shekhar K, Smillie C, Burgin G, Delorey TM, Howitt MR, Katz Y, Tirosh I, Beyaz S, Dionne D, Zhang M, Raychowdhury R, Garrett WS, Rozenblatt-Rosen O, Shi HN, Yilmaz O, Xavier RJ, Regev A. 2017. A single-cell survey of the small intestinal epithelium. Nature 551:333–339. https://doi.org/10.1038/nature24489.
83. Ye L, Bae M, Cassilly CD, Jabba SV, Thorpe DW, Martin AM, Lu H-Y, Wang J, Thompson JD, Lickwar CR, Poss KD, Keating DJ, Jordt S-E, Clardy J, Liddle RA, Rawls JF. 2021. Enteroendocrine cells sense bacterial tryptophan catabolites to activate enteric and vagal neuronal pathways. Cell Host Microbe 29:179–196. https://doi.org/10.1016/j.chom.2020.11.011.
84. Shiraki T, Koshimura K, Kobayashi S, Miwa S, Masaki T, Watanabe Y, Murakami Y, Kato Y. 1996. Stimulating effect of 6*R*-tetrahydrobiopterin on Ca^{2+} channels in neurons of rat dorsal motor nucleus of the vagus. Biochem Biophys Res Commun 221:181–185. https://doi.org/10.1006/bbrc.1996.0566.
85. Ciosek J, Guzek JW. 1992. Neurohyophysial function and pteridines: effect of (6*R*)-5,6,7,8-tetrahydro-α-biopterin on bioassayed hypothalamo-neurohypophysial vasopressin and oxytocin in the rat. Folia Medicia Cracoviensia 33:25–35.
86. Ciosek J, Guzek JW, Orłowska-Majdak M. 1992. Neurohypophysial vasopressin and oxytocin as influenced by (6*R*)-5,6,7,8-tetrahydro-α-biopterin in euhydrated and dehydrated rats. Biol Chem Hoppe Seyler 373:1079–1083. https://doi.org/10.1515/bchm3.1992.373.2.1079.
87. Bonaz B, Bazin T, Pellissier S. 2018. The vagus nerve at the interface of the microbiota-gut-brain axis. Front Neurosci 12:49. https://doi.org/10.3389/fnins.2018.00049.
88. Stromeck A, Hu Y, Chen L, Gänzle MG. 2011. Proteolysis and bioconversion of cereal proteins to glutamate and γ-aminobutyrate (GABA) in rye malt sourdoughs. J Agric Food Chem 59:1392–1399. https://doi.org/10.1021/jf103546t.
89. Silverman JL, Yang M, Lord C, Crawley JN. 2010. Behavioural phenotyping assays for mouse models of autism. Nat Rev Neurosci 11:490–502. https://doi.org/10.1038/nrn2851.
90. Bitto A, Ito TK, Pineda VV, LeTexier NJ, Huang HZ, Sutlief E, Tung H, Vizzini N, Chen B, Smith K, Meza D, Yajima M, Beyer RP, Kerr KF, Davis DJ, Gillespie CH, Snyder JM, Treuting PM, Kaeberlein M. 2016. Transient rapamycin treatment can increase lifespan and healthspan in middle-aged mice. Elife 5:e16351. https://doi.org/10.7554/eLife.16351.
91. Bariselli S, Tzanoulinou S, Glangetas C, Prévost-Solié C, Pucci L, Viguié J, Bezzi P, O'Connor EC, Georges F, Lüscher C, Bellone C. 2016. SHANK3 controls maturation of social reward circuits in the VTA. Nat Neurosci 19:926–934. https://doi.org/10.1038/nn.4319.
92. Zhang TA, Placzek AN, Dani JA. 2010. *In vitro* identification and electrophysiological characterization of dopamine neurons in the ventral tegmental area. Neuropharmacology 59:431–436. https://doi.org/10.1016/j.neuropharm.2010.06.004.